

Wind Intensity and Power Density in the Brazilian Dry Tropical Forests (Caatinga)

Madson Tavares Silva (✉ madson.tavares@ufcg.edu.br)

Universidade Federal de Campina Grande <https://orcid.org/0000-0003-1823-2742>

Welinagila Grangeiro de Sousa

Federal University of Campina Grande: Universidade Federal de Campina Grande

Enilson Palmeira Cavalcanti

Universidade Federal de Campina Grande

Vicente de Paulo Rodrigues da Silva

Universidade Federal de Campina Grande

Edivaldo Afonso de Oliveira Serrão

Universidade Federal de Campina Grande

Research Article

Keywords: Semiarid Region, Wind Speed, Wind Direction, Wind Potential

Posted Date: June 16th, 2021

DOI: <https://doi.org/10.21203/rs.3.rs-530683/v1>

License:   This work is licensed under a Creative Commons Attribution 4.0 International License.

[Read Full License](#)

Abstract

Wind speed has been widely used for energy purposes. Therefore, studies focused on its knowledge are extremely relevant to better benefit from this resource. The aim of this study is to analyze wind behavior and estimate wind power density (WPD) in the interior of northeastern Brazil, a region with predominance of the semi-arid climate, based on the data made available by the automatic station installed at the Experimental Farm in the municipality of São João do Cariri-PB, which come from the SONDA project and refer to the year 2007. Descriptive analysis techniques were used to identify the periods in which the wind behavior is more favorable to wind harnessing. From the results obtained, there was a predominance of southeast in the wind direction component. However, the values of both the observed wind speed (2, 25 and 50 m) and the wind speed estimated for the levels of 100 and 150 m, as well as the estimates of power density (50, 100 and 150 m) showed that the lowest records are present mainly in the first hours of the day, as well as in the first half of the year, while the highest values occur from 10 a.m. extending to the beginning of the night and prevail in the last six months of the year. These determinations denoted higher values of wind power density available for the second half of the year (mainly from August to December).

Highlights

1. The direction and speed wind is analyzed for hourly, monthly and seasonal at different heights
2. The surface wind speed is seasonal, with higher values in the last six months of the year.
3. The highest wind speeds at 100 and 150 m altitude occur in the dry season.
4. The greatest potential for wind energy at the 50, 100 and 150 m levels occurs between winter and summer in the region.

1. Introduction

Derived from the horizontal gradients of atmospheric pressures, wind is a meteorological element that has been investigated for decades by several authors, in order to better understand its behavior (Jing et al., 2020).

Both energy resources and their applications require studies that provide increasingly detailed knowledge. This practice leads to a better profit and more sustainable use of natural resources, in order to meet human needs, without depriving generations who will benefit from the same resources (Lopez, 2012). In this context, according to Mariano et al. (2017), one of the most promising renewable energies with the least impact on the environment is obtained from the wind.

Sauer et al. (2006) state that Brazil has excellent sites for the implementation of wind parks, and the best areas are found along the coast. However, these authors indicate that sites with capacity for wind power

generation are located in the interior, particularly in the Northeast region, where the state of Paraíba is situated. In addition, Oliveira and Costa (2011) assume that the geographic favoritism of the Brazilian Northeast (NE) with the intensity and constancy of the trade winds provide adequate conditions for the exploitation of this resource as an energy alternative.

The availability of updated information from local and regional wind fields is essential for efficient management and forecasting of wind energy production (Perez et al., 2014). For the installation of wind turbines, it is essential to conduct a preliminary study to obtain the local wind potential, such as the intensity of wind speed and direction.

Several authors have studied the wind potential existing in the Brazil territory. In their work Lima and Filho, (2010), these authors characterized the wind regime in the region of Triunfo, Pernambuco and found predominance of winds from the Southeast, using data obtained from the SONDA (*Sistema de Organização Nacional de Dados Ambientais*) Project. However, the values showed a wind potential above the average found in other places inside and outside Brazil.

Through statistical treatment of wind data for the year 2008, Alé et al. (2010) performed the wind characterization of the microregion of São João do Cariri-PB. The authors estimated the average annual wind speed at 100 m. However, they concluded that the site is not attractive for a large wind parks, but could be a useful region for the installation of small turbines. Results similar to those of the aforementioned authors were found by researchers Lima and Filho, (2012) when analyzing the wind resources of São João do Cariri-PB, through data from the SONDA project for the period from 2006 to 2009 at levels of 25 and 50 m.

The results of studies on wind resources depend on the quality of the available data, and these studies can provide only an approximation of the overall potential of wind energy. In addition, it is important to consider that the potential for wind energy can vary significantly for different regions (Hernandez-Escobedo et al., 2011; Manzano-Agugliaro et al., 2013).

Paraíba has favorable meteorological and relief conditions for wind harnessing both in coastal areas and inland areas. Based on this, this study aims to present, through a case study for the region of São João do Cariri-Paraíba, the behavior of wind speed at different heights, as well as the estimation of wind power density in this locality at levels of 50, 100 and 150 m.

2. Methodology

2.1. Study Area

The municipality of São João do Cariri is located in the *Borborema* Mesoregion and in the *Cariri Oriental Paraibano* Microregion has a total area of 653.09 km², being occupied by 4,344 inhabitants with a population density of 6.65 inhabitants/km², according to the last census. The municipality is bordered by Gurjão and Santo André to the North; Parari, Serra Branca and Coxixola to the West; Cabaceiras and São

Domingos do Cariri to the East, and Caraúbas to the South. It is 186.6 km away from the state capital, João Pessoa (Medeiros et al., 2015). Fig. 1 shows the location of the city of São João do Cariri-PB.

2.1.1. Climate and Relief

According to Köppen's classification, the climate is Bsh (hot semiarid), with highly variable rainfall in its spatial, temporal and interannual distribution, and a dry season that can reach up to 11 months (Araújo et al., 2005). *Cariri Oriental* has an average rainfall ranging from 400 to 500 mm year⁻¹ and relative humidity of approximately 70%. The temperature ranges from 27.2 °C in the November-March period to 23.1 °C in July, which are the maximum and minimum values, respectively (Sousa et al., 2007).

The geology of the area in which the municipality is situated consists of the crystalline basement of Precambrian age, where gneisses, migmatites and granites predominate. The site under study is located in the physiographic zone of the *Borborema* Plateau, in the *Borborema* mesoregion and *Cariri Oriental* microregion, with a predominantly flat and gently undulating relief, where the area is located on a surface of the Paraíba's territory intensely lowered by erosion cycles initiated at the end of the Tertiary Period, which have peripherally cut the Northeast portion of the Brazilian shield, with altitudes ranging between 400 and 600 m (Andrade-Lima, 1981; Araujo et al., 2011).

The predominant vegetation is of the hyperxerophilic Caatinga type according to Sousa et al. (2007), and the most commonly found species are: 'jurema preta' (*Mimosa tenuiflora* Willd. Poiret.), 'pereiro' (*Aspidosperma pyrifolium* Mart.), 'catingueira' (*Caesalpinia pyramidalis* Tul), 'angico' (*Anadenanthera columbrina* Vell. Brenan), 'aroeira' (*Myracrodruon urundeuva* Allemão) and various cactus species.

2.2. Data Used

Observed data of wind speed and direction at 2 m height, with records every 15 minutes were used, but considering only those arranged in hourly averages for the year 2007 obtained from the automatic station installed in the "Bacia Escola" Experimental Farm (Araujo et al., 2005), belonging to and made available by the Federal University of Campina Grande.

The study of this area also used the records from the anemometric tower located in the Experimental Farm, made available by the SONDA (*Sistema de Organização Nacional de Dados Ambientais*) project of INPE (*Instituto Nacional de Pesquisas Espaciais*). The main objective of the SONDA project is to develop a physical and human resource infrastructure to create and improve the surface database necessary for the survey of solar and wind energy resources in Brazil, and the consequent planning of their use (Martins et al., 2008).

The SONDA data network, before making the data of its stations available, subjects them to a validation process that aims to identify suspicious data. The data validation processes obtained by SONDA stations are based on the data quality control strategy adopted by BSRN (*Baseline Surface Radiation Network*).

Although BSRN deals only with solar radiation, its data control strategy has also been applied to meteorological and anemometric data (SONDA, 2019).

The data of the anemometric station (SONDA), available for the twelve months of the year used in the study (lack of records in May), include the year 2007, obtained at heights of 25 m and 50 m, with records every 10 minutes. However, this analysis considered only the data of wind speed and direction, organized in hourly averages.

2.3 Methods

2.3.1. Data Processing

For the modeling addressed in this study, electronic spreadsheets were used to estimate and organize the data, as well as the programming language R (R Core Team, 2019), through the use of openair and dplyr packages.

2.3.2. Descriptive Analysis

The data were described by means of central tendency (mean, median) and dispersion (standard deviation), as well as frequency density.

2.3.3. Wind Speed Estimation

Wind data were measured at heights of 2, 25, and 50 m. For this reason, a logarithmic expression was used to estimate wind speed at heights of 100 and 150 m, Eq. (1). More details can be obtained in Manwell et al. (2002).

$$V(z) = V(z_r) \frac{\ln \frac{z}{z_0}}{\ln \frac{z_r}{z_0}} \quad (1)$$

where:

$V(z_r)$ is the wind speed (m/s) at the reference height, considered as 25 m;

$V(z)$ is the wind speed (m/s) at the desired height;

z is the desired height (m);

z_r is the reference height (m) and

Z_0 is the roughness (m) of the region.

The roughness coefficient value for the terrain used in the study was 0.15 m, according to the criteria indicated in Table 1 (Fernandez Diez, 2003).

Table 1. Roughness coefficients (m) as a function of the type of terrain.

Terrain Description	Coefficients
Flat areas with ice or forest	0.08-0.12
Flat areas (sea, coast)	0.14
Slightly rugged terrains	0.15-0.16
Rustic zones	0.20
Rugged terrains or woodland	0.20-0.26
Highly rugged terrains and city	0.25-0.40

2.3.4. Wind Power Available in the Wind

Wind energy arises from the potential energy in the wind, which is transformed into circular motion energy that passes through the blades connected to the rotor and is converted into electric energy (Martins et al., 2008), thus constituting the basic operation principle of wind turbines. The equation of available wind power is expressed by Eq. (2) according to Custódio (2009).

$$P_{available} = \frac{1}{2} \rho AV^3 \quad (2)$$

where: $P_{available}$ is the available wind power perpendicular to the speed (m/s) to the cube; A is the area given in meters (perpendicular to the wind), formed by the rotational diameter of the blades of the wind turbines through which the wind passes, and ρ (kg/m^3) is the air density

However, Physicist Albert Betz determined an index that explains the total use of the energy available in the wind, which is approximately 59%. This factor was called Betz Power (Betz, 1926). This power expresses the losses caused by the dissipation of mechanical energy in wind turbines, among other factors. Thus, through mathematical reorganizations in Eq. (2), it was observed that wind power density (WPD) is given by the available power divided by the cross-sectional area, which results in the following equation:

$$D_p = \frac{P_{available}}{A} = \frac{1}{2} \rho V^3 \quad (3)$$

where:

ρ (kg/m³) is the air density; and

V is the speed (m/s).

3. Results

3.1. Wind Variability and Temperature at 2, 25 and 50 m Heights

Figure 2 shows the hourly and monthly behavior of wind speed, for the year 2007, in the region of São João do Cariri at levels close to the surface, heights of 2, 25 and 50 m.

The variability of wind speed at the level of 2 m (Fig. 2) has higher intensity in the daytime (09:00 to 18:00 h) with an average of around 4.5 m/s. However, the lowest values of wind speed occur in the interval between the night and early morning. It is also worth mentioning that wind speed averages below 4.5 m/s were recorded throughout the studied year.

The influence of the surface is especially dominant in a layer comprising the first 50–100 m of the atmosphere, where heat and humidity exchanges occur between the surface and atmospheric air, mainly due to the availability of radiation from the Sun (Martins et al., 2008).

The trend of daytime winds greater than those at night occurs because the surface heating process causes great variability throughout the day and a predominance of higher intensities in the daytime, so the wind potential also undergoes changes in the daytime regime (Oliveira et al., 2004; Oliveira e Souza, 2018).

Thus, by analyzing the variability of wind speed at levels of 25 and 50 m (Fig. 2), it can be noted that the speed profile (hourly and monthly averages) for both exhibits similar behavior. As for the hourly variation, the greater variability of wind speed is noticeable during the morning, but with the lowest averages for both levels. The highest wind speeds occur in the afternoon, where the maximum peak for both levels is at 18:00 h (6.8 m/s for 25 m and 8 m/s for 50 m), thus corroborating the classical pattern with occurrences of the highest magnitudes of wind speed during the day (Junior et al., 2010). Martins et al. (2008) points out that at greater heights the friction on the wind is lower, so higher speeds are reached compared to those at lower heights, exponentially increasing the speed as a function of the increase in height.

The highest wind speed intensities throughout the Northeast occur in the second half of the year (Nóbrega and Aquino, 2009). In line with the cited authors, Lima and Filho (2012), when analyzing the wind in the same locality in question for the period from 2006 to 2009, obtained values consistent with

those found in the current study, with lower values of wind speed in the first half (March-April-May) and higher values in the second half (November).

In a related study for five regions of Paraíba, Lima et al. (2010) found similar results, with the presence of maximum wind speeds in the second half of the year.

More intense winds in the night time is a typical characteristic of regions farther from the coast (Germano and Junior, 2016). Therefore, this fact may explain the occurrence of stronger winds during the night time in São João do Cariri for some months of the year.

It worth pointing out that the greater the temperature variation in a given region or place, the greater the wind circulation (Silva et al., 2012). The magnitude of these variations is directly dependent on weather conditions as well as local conditions (Oliveira, 2011).

Based on this assumption, the average hourly and monthly variation in air temperature in São João do Cariri in 2007 is presented in Fig. 3. The four seasons of the this year show temperature variations, especially during the day, when the winds are commonly stronger from a certain time, characterizing a high variation in their intensities during the year at some heights.

It was observed that the air temperature at 2 m height begins to increase from 6:00 h, with “high” values between 12:00 and 18:00 h, and the highest thermal gradient occurs at 15:00 h (31°C), as shown in Fig. 3. Reboita et al. (2016) states that the temperature varies greatly with altitude and this difference in its behavior originates in the way through which each of its layers is heated.

Thus, it was observed that at levels of 25 and 50 m there is a behavior of increase in the values of air temperature, possibly caused by the greater supply of solar energy, and for the period from 7:00 to 18:00 h, the process of heating of the upper layers of the surface result in a higher availability of stored heat around 18:00 h for both levels, with records of 29°C for 25 m and 28.5°C for 50 m, agreeing with the time at which there is a sudden increase in wind speed intensities for the same heights (Fig. 2).

It is also observed that the minimum values of air temperature for the three heights are recorded in the months of May, June, July and August, with the minimum peak observed in August (around 22°C). Over the course of the other months, the temperature begins to rise significantly. The maximum values occur between October and February, with maximum value in January: 26.5°C for 2 m, 26.2°C for 25 m and 25.8°C for 50 m. The maximum values of air temperature are directly related to the high solar radiation.

Temperature variations as a function of height are responsible for the intensity of turbulence; the closer to the surface the more intense, due to natural factors. As height increases, it is induced mainly by convection (Montanher e Minaki, 2018).

3.2. Seasonal analysis of wind direction

Another key aspect to studying the wind, besides its speed, is its direction. It is essential to know this aspect in order to determine the optimization of the use and consequently its maximization in the

generation of energy.

Figure 4 shows the possible seasonal wind directions for the municipality of São João do Cariri at the three heights under study in 2007. It is noted that for the level of 2 m the predominant wind direction in all seasons is between 100 and 150° (East-Southeast and South-Southeast). For the height of 25 m, the dominant seasonal direction for the whole year is between 150 and 200° (South-Southeast and South-Southwest). At 50 m height, the directions are similar to those for 25 m (South-Southeast and South-Southwest), with a greater predominance also from 150 to 200° for all seasons.

An analysis reveals that, for the three levels evaluated in the region of São João do Cariri, there is greater variability in direction in the summer and autumn seasons, when compared to the predominant direction.

Variations in wind direction can occur on the same time scale as variations in wind speed. Seasonal variations in wind direction can be small, around 30°, or exceed 180°. Sudden changes in direction may also occur due to the turbulent behavior of the air due to height (Foley et al., 2012).

When studying the direction regime for São João do Cariri-PB in the period from 2006 to 2009, some authors Lima and Filho (2012), obtained results of direction similar to those found at the three heights analyzed, predominantly southeast, with seasonal variations.

By observing the average monthly variation of wind direction for five regions of the Paraíba state (São Gonçalo, Monteiro, Patos, Campina Grande and João Pessoa), Lima et al. (2010) found similar results to those found here, with wind direction in the regions varying between the angles of 20° and 180° in the study period. In an analogous study for the Sub-middle São Francisco River, Lopes et al. (2017) found a predominant frequency in the southeast direction for the winds in the region.

3.3. Estimates of wind speed at heights of 100 and 150 m

As height increases in the atmosphere, friction is reduced and the wind reaches greater speed, so it is important to analyze the wind regime at several different levels.

From the average wind speed in the site at 25 m height, the speeds for the heights of 100 and 150 m were estimated in order to verify the wind behavior at different levels, which are considered of interest for energy use because they undergo lower alterations due to relief conditions, presence of obstacles and vertical thermal stability (CEMIG,2010).

As energy production is highly dependent on wind speed, assessing its variability is extremely relevant. As the height increases, the frictional force contrary to the direction of airflow is reduced, increasing the intensity of wind speeds (Silveira et al., 2000; Paula et al., 2017).

Figure 5 shows the hourly and monthly variations of wind speeds for the two heights at which they were estimated (100 and 150 m). It can be noted that the greatest variability of wind speed (shaded area) occurs during the day, for both 100 and 150 m. Wind intensity has greater oscillation in the daytime possibly due to the thermal variability in the site.

It is noted that the wind speed begins to decrease in the early morning extending until 6:00 h (with average of around 3 m/s for both heights), from which there is a sudden increase. However, the highest values of wind speed comprise the time interval from 9:00 to 19:00 h, the highest peak of which is seen at 19:00 h, reaching 8.8 m/s for 100 m and 9.5 m/s for 150 m.

At levels closer to the earth's surface, the interval of greatest magnitude of the wind occurs during the day, from dawn to late afternoon, and the strong thermal gradient generated by surface heating is the main mechanism for this condition. However, with the increase in height, there is a variation in this cycle, and the wind at night starts to gain speed over a certain period (Arya, 2001; Lyra and Pereira, 2007).

For elevations greater than 50 meters, the effects of the surface on the wind are already smaller and synoptic scale mechanisms act with greater intensity. Commonly, the daytime evolution of wind is reversed at high levels (above 100 meters), with higher peaks of speed in the night time (Arya, 2001).

The levels of wind speed variability in some wind parks installed in the interior of Bahia denote similarities with the characteristics of the wind in São João do Cariri, where the winds blow with less intensity during the early morning and with greater intensity after sunset (AMA, 2013).

Regarding the monthly variability for the heights under discussion, the highest values comprise the four-month period from August to November, with averages ranging from 7 to 8 m/s for 100 m and 8.5 to 9 m/s for 150 m (Fig. 5). From December, wind speeds begin to decrease, with lower values occurring in the six-month period from February to July, ranging from 5.3 to 5.9 m/s for 100 m and 5.7 to 6.2 m/s for 150 m. In the rainy season (February to May), the occurrence of precipitation can change the average hourly intensities of wind speed.

Similar average values were found by Mariano et al. (2017) when analyzing the wind speed in the regions of *Agreste*, *Borborema* and *Sertão* of Paraíba, at heights of 10, 70 and 100 m. The values were more intense at levels of 70 and 100 m. Analyzing the daily wind speed cycle for a locality in the state of Ceará, Lima et al. (2011) observed low values in the early morning period (between 1:00 and 7:00 local time) and high values in the period between 10:00 and 18:00 local time. Maximum values are observed at night time where there are local mesoscale circulations, such as land breezes.

Oliveira and Sousa (2018), when analyzing the wind behavior in the mesoregions of Paraíba, highlighted *Borborema* as the region where the wind is most intense, with specific areas to the north and south (where São João do Cariri is located).

For wind exploitation to be viable in a given area, wind speeds of 3.0 m/s are required for small turbines and 6.0 m/s for large turbines. Below these values, the energy content of the wind does not justify its use (Rüncos et al., 2005). Therefore, based on the estimated average values for the two levels, São João do Cariri theoretically has favorable wind conditions to the use of wind for energy purposes.

3.4. Estimates of power densities at 50, 100 and 150 m heights

In most places on the planet the wind blows more intensely during the day than at night, as a result of temperature differences, but it is more turbulent and subjected to variations in direction during the day (Oliveira, 2011).

The highest values of WPD are between August and December at the studied heights (Figs. 6, 7 and 8). During the winter, which is from June to September, the Northeast of Brazil has a high power density, and this characteristic still persists between the months from September to December due to the influence of southeast winds during this season (Silva et al., 2016).

By separately analyzing the power density at each level, it can be observed that at 50 m, Fig. 6, the mean values are 150 W/m^2 , being around the average found by Mariano (2017), when verifying the WPD for the *Borborema* region (where São João do Cariri is located) at height of 70 m (182 W/m^2). This average value is identified along the entire year, but is more present in the first six months, especially in the afternoon. Regarding the highest values (from 300 to 500 W/m^2), they are present from August to mid-February, ranging from 09:00 to 22:00 h. However, the maximum values are present in October, November and December (all within the range from 18:00 to 21:00 h).

For the level of 100 m, Fig. 7, the average power density found, equal to 230 W/m^2 , was very close to the average value obtained for the same height, 224 W/m^2 , for the mesoregion where the analyzed locality is located (Mariano, 2017).

The lowest values of WPD (below 200 W/m^2) comprise the time interval from 00:00 to 07:00 h throughout the year 2007. Maximum values (500 to 700 W/m^2) start from August to January. However, in August and September these values vary from morning to evening (09:00 to 20:00 h), unlike the other months, where these maximums occur from late afternoon (17:00 to 21:00 h), due to higher values of wind speed, as already mentioned.

In an equivalent study, Lima et al. (2010) analyzed the wind power density for winds at 110 m height for some stations, including that of Patos, and observed average values similar to those found for the region of São João do Cariri. These authors state that in the interior of Paraíba it is assumed that there is great orographic influence in all regions, and low values of power are observed at heights close to the surface.

Figure 7. Wind power density (WPD) for the 100 m level.

At 150 m height, Fig. 8, the mean WPD was 276 W/m^2 , and the minimum values (from 100 to 200 W/m^2) vary throughout the day in the first half of the year; however, in the second half they are more frequent in the hours from midnight until the early morning (00:00 to 07:00 h). The maximum values (500 to 900 W/m^2) start in August and continue until January. However, their time regimes follow the same pattern as those of previously analyzed heights.

It is worth pointing out that the maximum wind energy production in the second half, according to the WPD, coincides with the dry season in the region and consequently with the period of lower water

availability in the production of hydroelectric energy in drought years (Becker et al., 2011). Thus, wind energy, if properly exploited, can supply this deficiency. On the other hand, in the first half, there are greater availability of hydroelectric energy in months of lower wind power, especially in rainy years. A similar pattern was observed among different regions of the Northeast in a study conducted by Pinto et al. (2017), who verified wind behavior throughout the NE, with higher values in the months from August to January and lower values from February to July.

Another parameter obtained with data treatment is the frequency distribution of the seasonal wind power densities for the heights of 100 and 150 m. Figures 9 and 10 show the frequency densities of WPD for certain ranges. The curve superimposed on the WPD ranges denotes the probability distribution, characterizing the amplitude of the distribution.

By separately analyzing the densities for each height, it can be observed that at 100 m (Fig. 9), in the summer season, the highest density is between 0 and 140 W/m², totaling about 45% of the events for the interval. In the autumn, the highest repetitions with almost 70% range from 0 to 180 W/m², and in the winter the most frequent values range from 0 to 150 W/m² with 52%, but in the spring the highest incidences are between 0 and 170 W/m², with 34% of the episodes in this interval. The highest levels of variability occur in the summer (0 to 1373 W/m²) and spring (0 to 1630 W/m²) seasons.

For the height of 150 m, Fig. 10, the greatest variability occurred in summer (0 to 1646 W/m²) and in spring (1 to 1956 W/m²), as observed for the height of 100 m. The summer had higher density between 0 and 170 W/m², with 46% of the events in the interval, and the smallest events for this season were between 1360 and 1530 W/m² with only one occurrence. In autumn the largest repetitions range from 0 to 210 W/m², with 70% of the observations, but the lowest values are present within the range from 840 to 2100 W/m².

In winter, the most successive values range from 0 to 180 W/m² with a predominance of 52%, whose minimum values occur between 1260 and 1800 W/m². Finally, spring has higher incidences of 0 and 200 W/m², with 34% of occurrences in this interval, and minimum incidences between 1400 and 2000 W/m².

4. Conclusions And Future Perspectives

It should be pointed out that the results of the present study necessarily have a preliminary nature, enabling the evaluation of important characteristics of hourly, monthly and seasonal variation of wind direction and speed at different heights, being of great relevance for the use of this variable.

As for the wind speed distribution pattern for the heights near the surface, they showed a similar behavior, with minimum values in the initial months of the year and maximum values in the last six months. The dominant directions found were from the southeast, with seasonal variations, for the levels near the surface.

In this context, the simulations generated for wind speeds at 100 and 150 m heights demonstrated that lower values occur mainly in the morning interval as well as for the rainy season of the region (February to May), while the highest values occur from 10:00 h in the morning until late afternoon and early evening, and predominate in the months from September to November (dry season).

Regarding the estimation of wind power density in this locality at the levels of 50, 100 and 150 m, it was possible to observe that the months of higher WPD were those from August to January (late winter, spring and early summer), encompassing the dry season in the region, while the lowest densities occurred during the morning throughout the year 2007, especially in the first six months.

These determinations showed, therefore, that the results obtained with the simulations generated integrate a relevant database for the evaluation of wind behavior in this locality for future studies.

Declarations

Acknowledgements

Welinagila Grangeiro de Sousa thankful to the Coordination for the Improvement of Higher Education Personnel (CAPES) for the scholarship granted to the first author.

References

1. Alé JAV, Oliveira CP, Lopes AMG, 2010. Caracterização eólica de microrregião utilizando torre meteorológica e ferramenta computacional. Anais: Seminário Nacional Sobre Engenharia do Vento – SENEV, Belo Horizonte
2. AMA (2013) Caracterização do Recurso Eólico e Resultados Preliminares de sua Aplicação no Sistema Elétrico. Available in: <http://epe.gov.br/sitespt/publicacoesdadosabertos/publicacoes/PublicacoesArquivos>. (Last access: 05 January 2020)
3. Andrade-Lima DA (1981) Domínios da Caatinga Bras Bot 4:149–153
4. Araújo KD, Andrade AP, Raposo RWC, Rosa O, P. R. O., JR, E. P (2005) Análise das condições meteorológicas de São João do Cariri no Semiárido Paraibano. Rev Dep Geoc 14:61–72. <http://dx.doi.org/10.5433/2447-1747.2005v14n1p61>
5. Araújo KD, Andrade AP, Raposo RWC, Rosa O, P. R. O., JR, E. P., 2005. Análise das condições meteorológicas de São João do Cariri no semiárido paraibano. Rev. Dep. Geo. 14, 61–72. <http://dx.doi.org/10.5433/2447-1747.2005v14n1p61>
6. Araújo KD, Dantas RT, Andrade AP, Parente HN (2011) Cinética de evolução de dióxido de carbono em área de caatinga em São João Do Cariri-PB RevÁrvore.35, 1099–1106. <https://doi.org/10.1590/S0100-67622011000600016>
7. Arya P, 2001. Introduction to Micrometeorology. Universidade de Washington, Seattle

8. Becker CT, Melo MMMS, Costa MNM, Ribero EPR, 2011. Caracterização climática das regiões pluviometricamente homogêneas do estado da Paraíba. Bras. Geog. Fís. 1, 286–299. <https://doi.org/10.26848/rbgf.v4.2.p286-299>
9. Betz A (1926) Wind-Energie und Ihre Ausnutzung durch Windmühlen. Vandenhoeck & Ruprecht, Universidade de Michigan, Michigan
10. CEMIG, Companhia Energética de Minas Gerais, 2010. Atlas Eólico de Minas Gerais. Minas Gerais
11. Custódio RS (2009) Energia eólica para produção de energia elétrica. Synergia. Rio de Janeiro
12. Fernández Díez P (2003) Energía Eólica. Departamento de ingeniería eléctrica y energética. Universidad de Cantabria
13. Foley AM, Leahy PG, Marvuglia A, Mckeoghy EJ (2012) Current methods and advances in forecasting of wind power generation. Renew Energ 37:1–8. <https://doi.org/10.1016/j.renene.2011.05.033>
14. Germano AS, Junior RSS (2016) Estimativa do potencial eólico do estado de Alagoas utilizando o modelo atmosférico WRF. Eletr Energ 6:18–26
15. Hernandez-Escobedo Q, Manzano-Agugliaro F, Gazquez-Parra JA, Zapata-Sierra A (2011) Is The wind a periodical phenomenon? the case of Mexico. Renew Sust Energ Rev15, 721–728. <https://doi.org/10.1016/j.rser.2010.09.023>
16. Jing, H., Liao, H., M.A, Cunming., Tao, Q., Jiang, J., 2020. **Field measurement study of wind characteristics at different measuring positions in aa mountainous valley.** *Exp. Therm. Fluid. Scienc.* **112**. <https://doi.org/10.1016/j.expthermflusci.2019.109991>.
17. Junior RSS, Lyra RFF, Silva AR, Ramos DNS, Rabelo FD, 2010. Mapeamento do potencial eólico do estado de Alagoas, utilizando o modelo WRF. Available in: <https://www.researchgate.net/publication/299288666>. (Last access: 06 November 2019)
18. Lima FJL, Cavalcanti EP, Souza EP, 2010. Avaliação do potencial eólico em cinco regiões do estado da Paraíba. Geografia. 27,138–153
19. Lima FJL, Guedes RVS, Silva APN, Silva EM (2011) Avaliação do potencial eólico no município de Jaguaruana, litoral cearense. Ciênc Nat 31:101–115. <https://doi.org/10.5902/2179460X9970>
20. Lima LA, Filho CRB, 2010. Wind energy assessment and wind farm simulation in Triunfo – Pernambuco, Brazil. Renew. Energ. 35, 2705–2713. <https://doi.org/10.1016/j.renene.2010.04.019>
21. Lima LA, Filho CRB (2012) Wind resource evaluation in São João do Cariri (SJC)– Paraíba, Brazil. Renew Sust Energ Rev 16:474–480. <https://doi.org/10.1016/j.rser.2011.08.011>
22. Lopes I, Cerqueira Júnior EP, Melo JMM, Leal BG (2017) Wind power generation potential in the San Francisco submiddle. J Envir Anal Progress 2:330–340. <http://dx.doi.org/10.24221/jeap.2.3.2017.1407.330-340>
23. Lopez RA (2012) Energia Eólica. Energia e Meio Ambiente. Artliber Editora, São Paulo, 366 pp
24. Lyra GB, Pereira AR (2007) Dificuldades de estimativa dos parâmetros de rugosidade aerodinâmica pelo perfil logaritmo do vento sobre vegetação esparsa em região semi-árida. Bras Geof 25:187–

197. <https://doi.org/10.1590/S0102-261X2007000200007>
25. Manwell JF, Mcgowan JF, Rogers AL (2002) *Wind energy explained: Theory, Design and Application*, Washington
26. Manzano-Agugliaro F, Alcayde A, Montoya A, Zapata-Sierra C (2013) Scientific production of renewable energies worldwide: an overview. *Renew. Sust Energ Rev* 18:134–143. <https://doi.org/10.1016/j.rser.2012.10.020>
27. Mariano EB (2017) *Simulação do modelo BRAMS para instalação de parque eólico no nordeste setentrional oriental do Brasil*, Tese. Campina Grande
28. Mariano EB, Cavalcanti EP, Beserra EA (2017) Análise comparativa da velocidade do vento simulado pelo BRAMS com dados observados e de reanálises. *Bras Meteorol* 32:269–276. <http://dx.doi.org/10.1590/0102-778632220160128>
29. Mariano EB, Cavalcanti EP, Beserra EA (2017) Análise comparativa da velocidade do vento simulado pelo BRAMS com dados observados e de reanálises. *Bras Meteorol* 32:269–276. <https://doi.org/10.1590/0102-778632220160128>
30. Martins FR, Guarnieri RA, Pereira EB (2008) O Aproveitamento da energia eólica. *Bras, Ensino Fís.* 1, 1304.1-1304.13. <https://doi.org/10.1590/S1806-11172008000100005>
31. Medeiros RM, Santos DC, Francisco PRM, Filho MFG, 2015. Análise hidroclimática da região de São João do Cariri-PB. *Edu. Agr. Sup.* 30, 59–65. <http://dx.doi.org/10.12722/0101-756X.v30n02a01>
32. Montanher OC, Cíntia Minaki C (2018) Condicionantes geográficos da temperatura do ar no estado do Paraná. *Ra'eGa* 45:250–267. <https://doi.org/10.5380/raega.v45i1.55070>
33. Nóbrega MMH, Aquino RRB (2009) Oferta de energia através da complementaridade sazonal hidro-eólica, 40. *PCH Notícias & SHP News*, pp 24–28
34. Oliveira JL, Costa AA, 2011. Estudo de variabilidade do vento em escala sazonal sobre o nordeste brasileiro utilizando o Rams: os casos de 1973–1974 e 1982–1983. *Bras. Meteorol.* 26, 53–66. <https://doi.org/10.1590/S0102-77862011000100006>
35. Oliveira PJ, Rocha JP, Fisch G, Kruijt B, Ribeiro JBM (2004) Efeitos de um evento de friagem nas condições meteorológicas na Amazônia: um estudo de caso. *Acta Amaz* 34:613–619. <https://doi.org/10.1590/S0044-59672004000400013>
36. Oliveira SS, Souza EP, 2018. Utilização de modelos de mesoescala como ferramenta inicial para o mapeamento eólico do estado da Paraíba. *Bras Meteo* 33, 459–471. <https://doi.org/10.1590/0102-77863333006>
37. Paula LP, Cardoso FAC, Cardoso RB, Cunha GPQ, Vieira EM (2017) Modelagem espacial da velocidade do vento a 50, 75 e 100 metros de altura para o estado de Minas Gerais, Brasil, empregando geoestatística. *Bras Geog Fís* 10:1281–1295. <https://doi.org/10.26848/rbgf.v10.4.p1281-1295>
38. Perez AA, Salas JCP, Rosa JJG, Fernández JMS, 2014. Regional wind monitoring system based on multiple sensor networks: a crowdsourcing preliminary test. *J Wind Eng Ind Aerod* 127, 51–58. <https://doi.org/10.1016/j.jweia.2014.02.006>

39. Pinto LIC, Lima FJL, Martins FR, Pereira EB, 2017. Análise de agrupamento na otimização de futuras aplicações de modelagem numérica na estimativa e previsão de recurso eólico. *Bras Geog Fís* 10, 1698–1711. <https://doi.org/10.26848/rbgf.v10.6.p1698-1711>
40. R Core Team (2019) A language and environment for statistical computing. Viena, Áustria: R Foundation for Statistical Computing. Available in: <http://www.r-project.org>. (Last access: 15 September 2019)
41. Reboita MS, Rodrigues M, Armando RP, Freitas C, Martins D, Miller G (2016) Causas da semiaridez do sertão nordestino. *Bras Climatol* 19:254–277. <http://dx.doi.org/10.5380/abclima.v19i0.42091>
42. Rüncos F, Carlson R, Kuo-peng P, Voltolini H, Batistela NJ, 2005. Geração de energia eólica tecnologias atuais e futuras. *Eletric. Moder.* 1, pp.1–15
43. Sauer IL, Queiroz MS, Miragaya JCG, Mascarenhas RC, Júnior AR Q., 2006. Energia renováveis: ações e perspectivas na Petrobrás. *Bahia Análise e Dados*. 16, 9–22
44. Silva AR, Pimenta FM, Assireu AT, Spyrides MHC (2016) Complementarity of brazil's hydro and offshore wind power. *Renew Sustain Energy Review* 56:413–427. <https://doi.org/10.1016/j.rser.2015.11.045>
45. Silva CR, Silva JV, Junior JA, Carvalho HP (2012) Radiação solar estimada com base na temperatura do ar para três regiões de Minas Gerais. *Bras Eng Agríc Ambient* 16:281–288. <http://dx.doi.org/10.1590/S1415-43662012000300008>
46. Silveira ICA, Schimidt ACK, Campos EJD, Godoi SS, Ikeda YA (2000) Corrente do Brasil ao largo da costa leste brasileira. *Bras Oceanog* 48:171–183. <https://doi.org/10.1590/S1413-77392000000200008>
47. SONDA, 2019. Sistema de Organização Nacional de Dados Ambientais, Available in: <http://sonda.ccst.inpe.br/>. (Last access: 09 de November 2019)
48. Sousa RF, Barbosa PM, Neto T, Carvalho PC, Sousa AP, Júnior SP, Alencar MLS (2007) Geotecnologia no estudo da evolução espaço-temporal da cobertura vegetal do município de São João do Cariri-PB. *EngAmb* 4:60–67

Figures

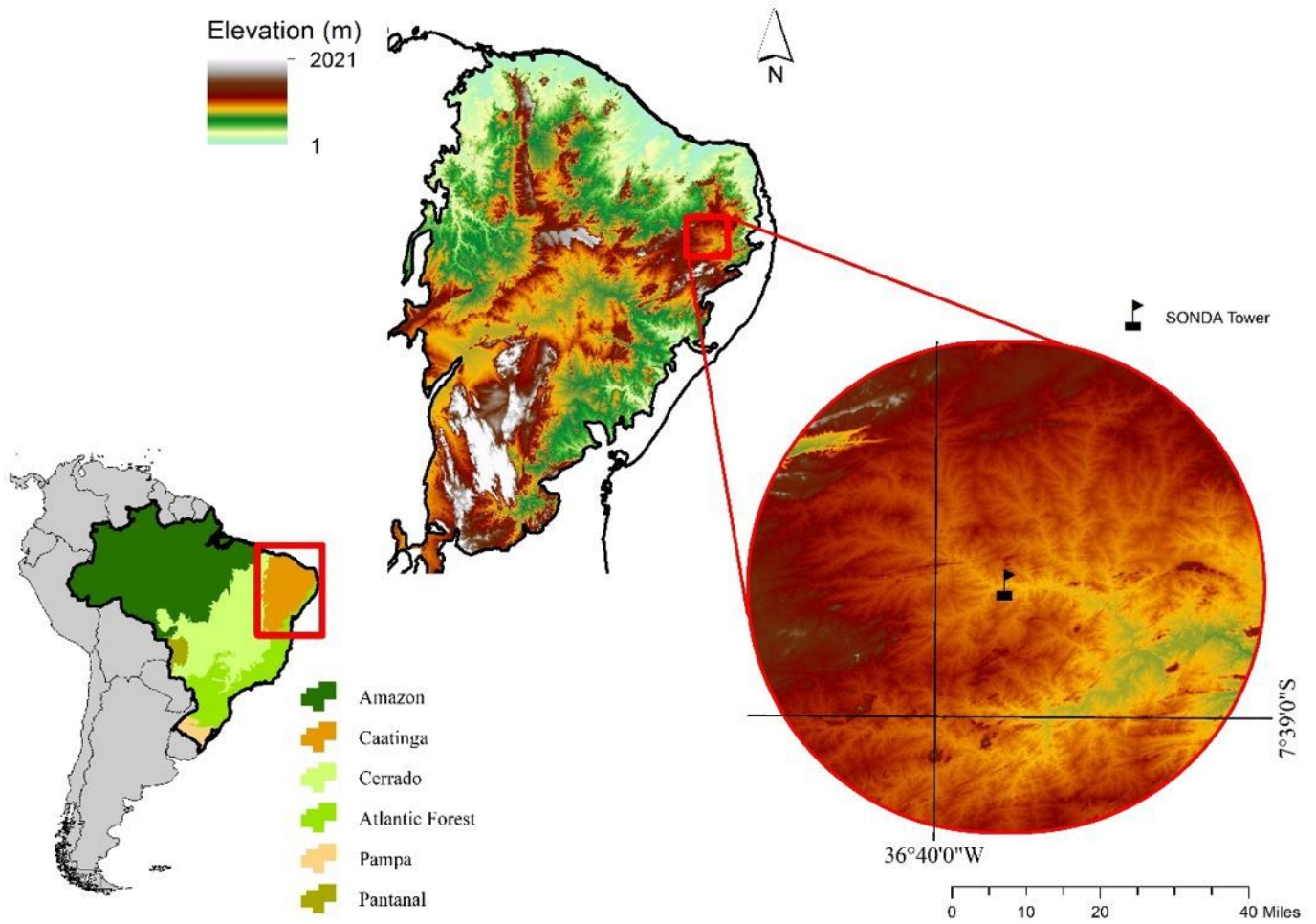


Figure 1

Study area location. Note: The designations employed and the presentation of the material on this map do not imply the expression of any opinion whatsoever on the part of Research Square concerning the legal status of any country, territory, city or area or of its authorities, or concerning the delimitation of its frontiers or boundaries. This map has been provided by the authors.

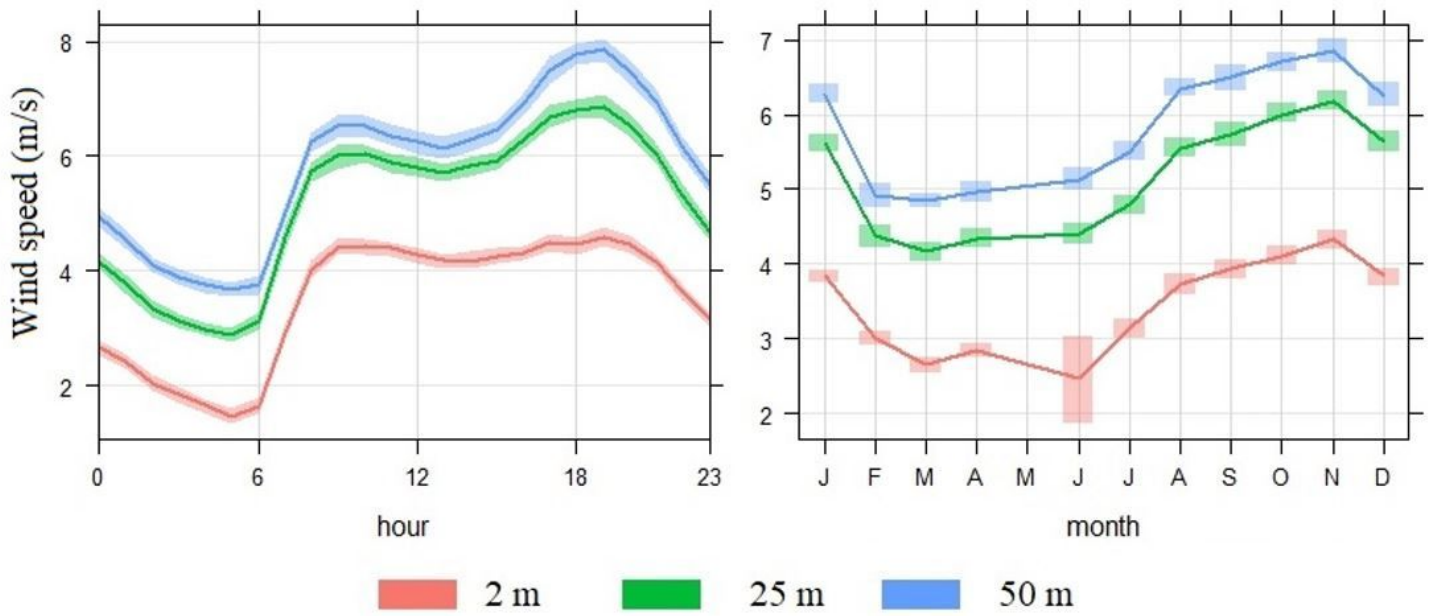


Figure 2

Hourly and monthly variability of wind speed for heights of 2, 25 and 50 m.

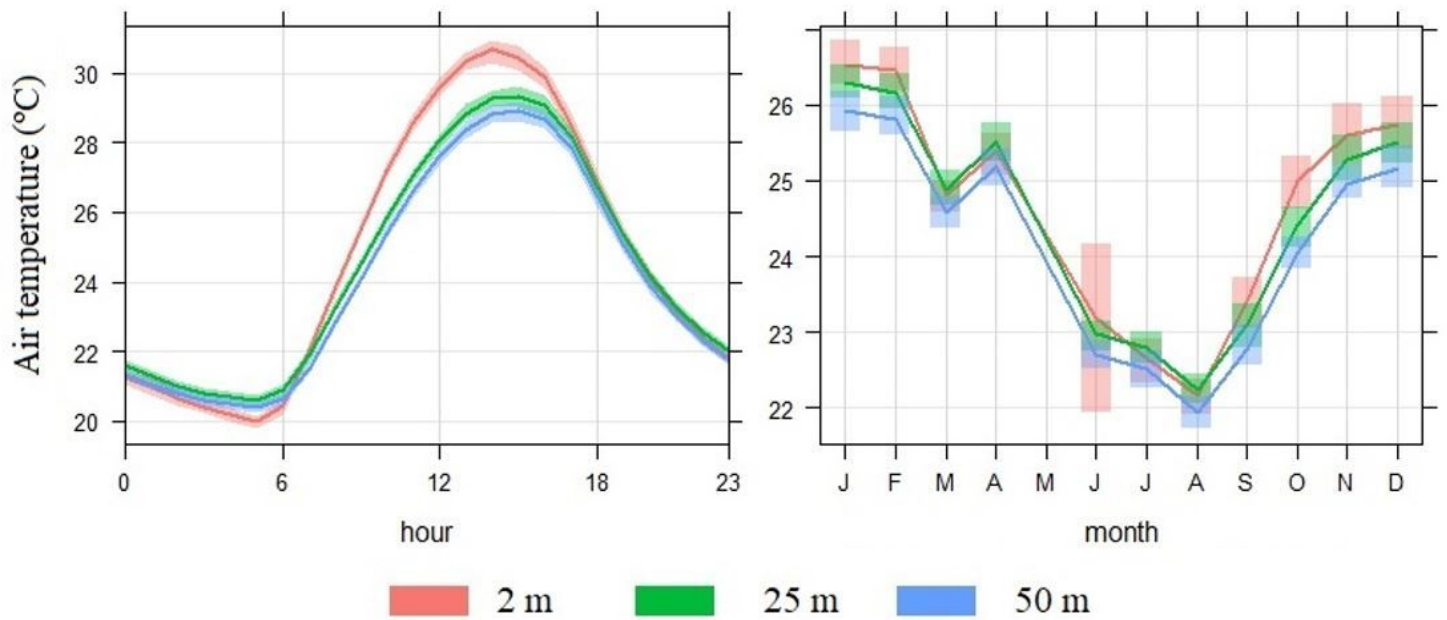


Figure 3

Hourly and monthly variability of air temperature for heights of 2, 25 and 50 m.

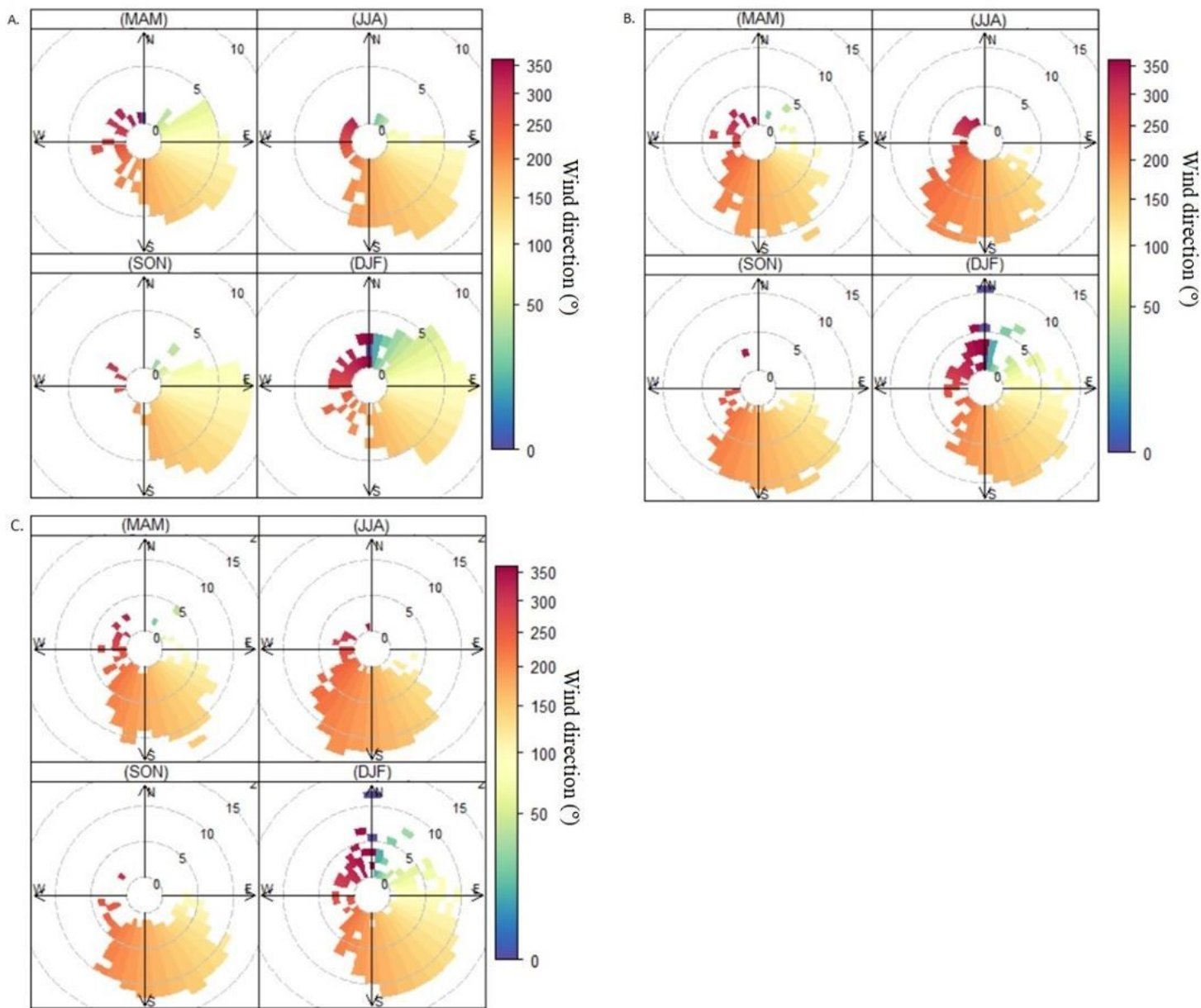


Figure 4

Seasonal variability of wind direction for heights of 2 m (A), 25 m (B) and 50 m (C).

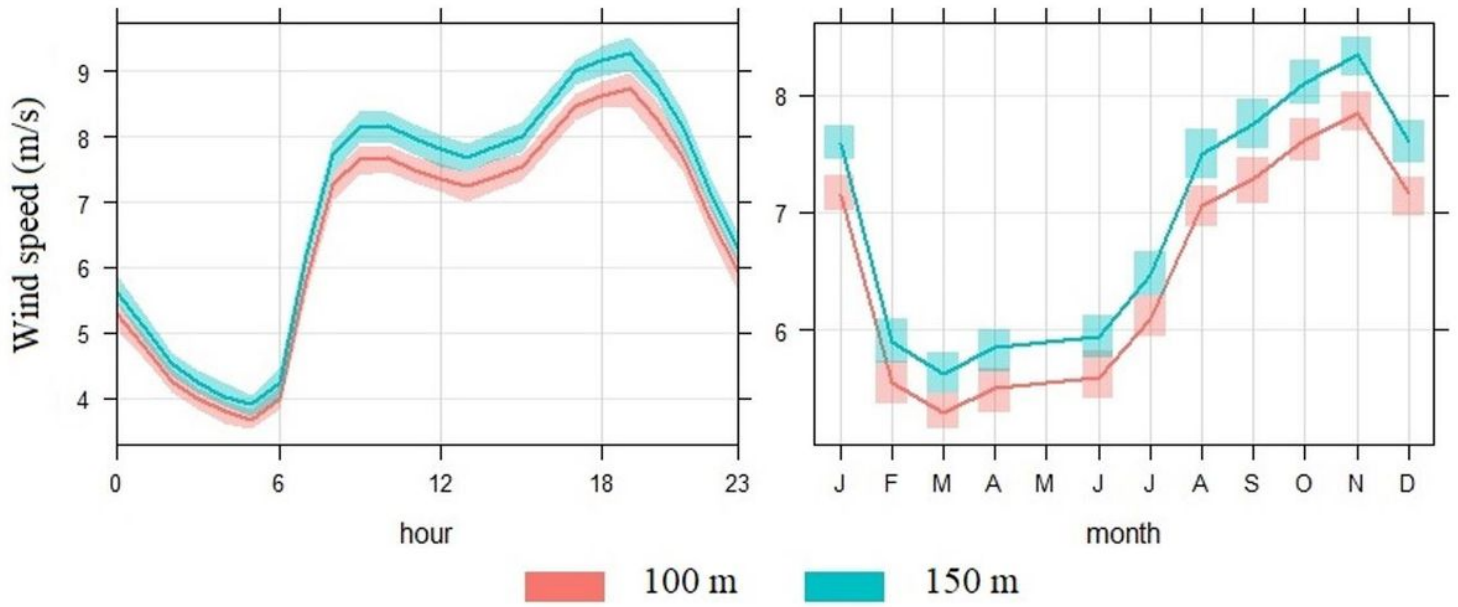


Figure 5

Wind speed variability for the levels of 100 and 150.

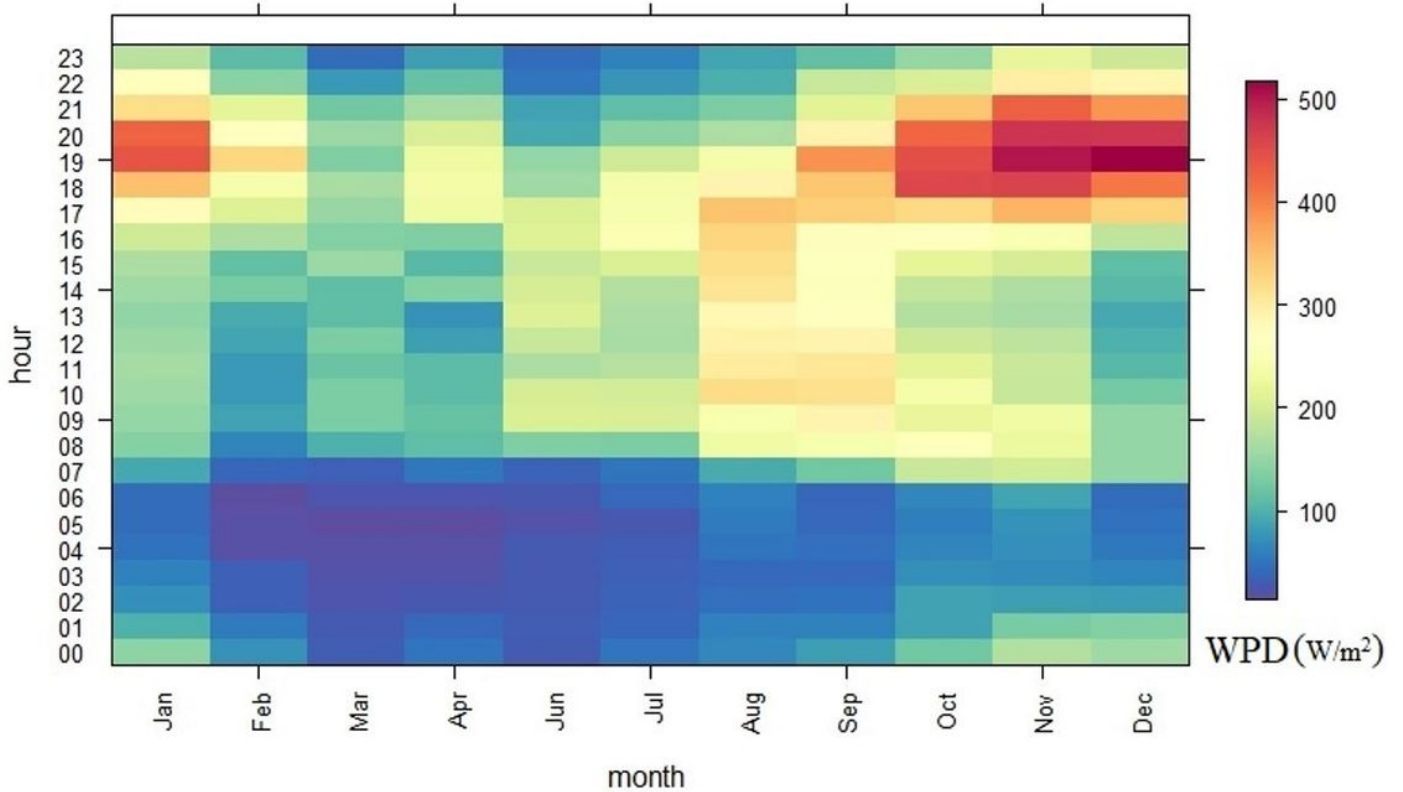


Figure 6

Wind power density (WPD) for the 50 m level.

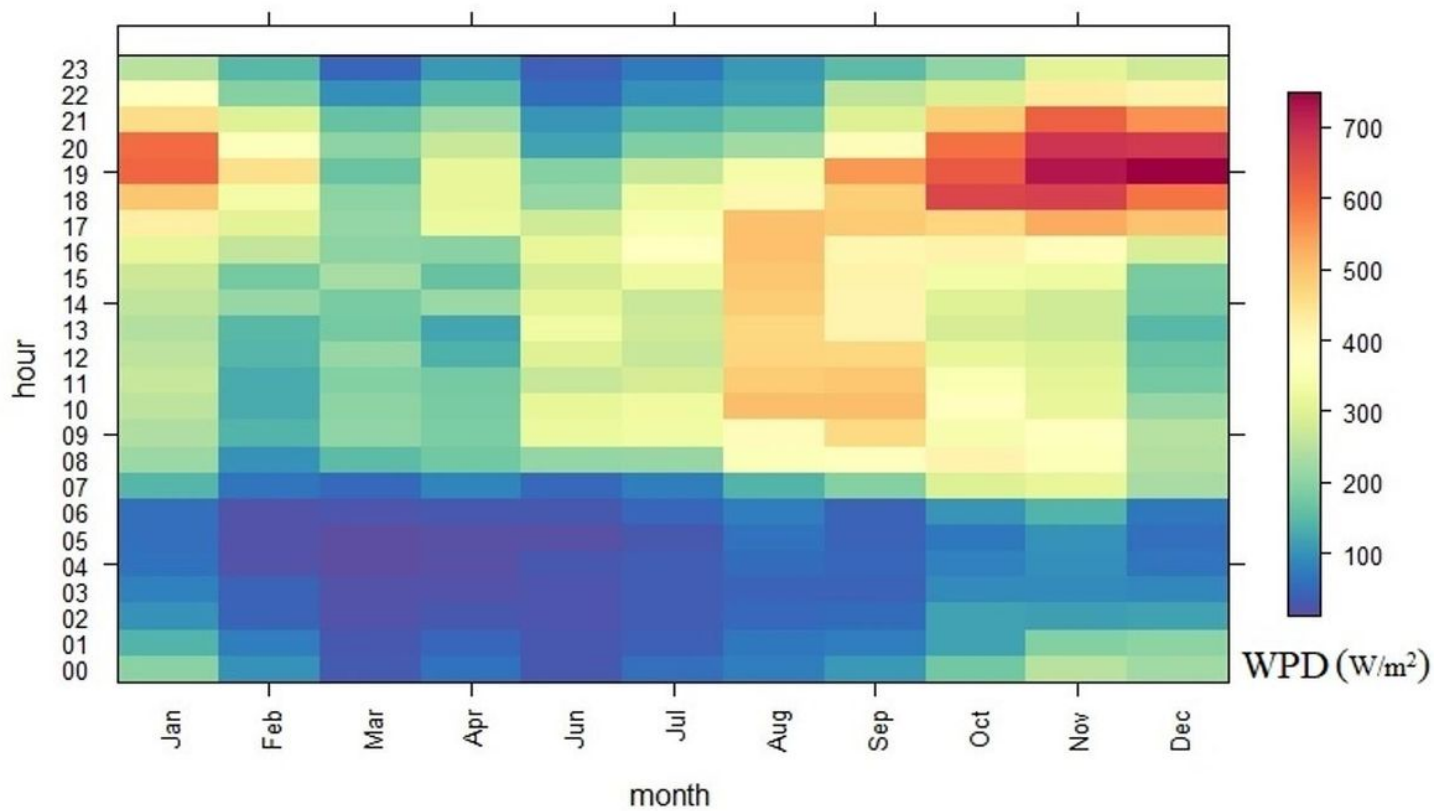


Figure 7

Wind power density (WPD) for the 100 m level.

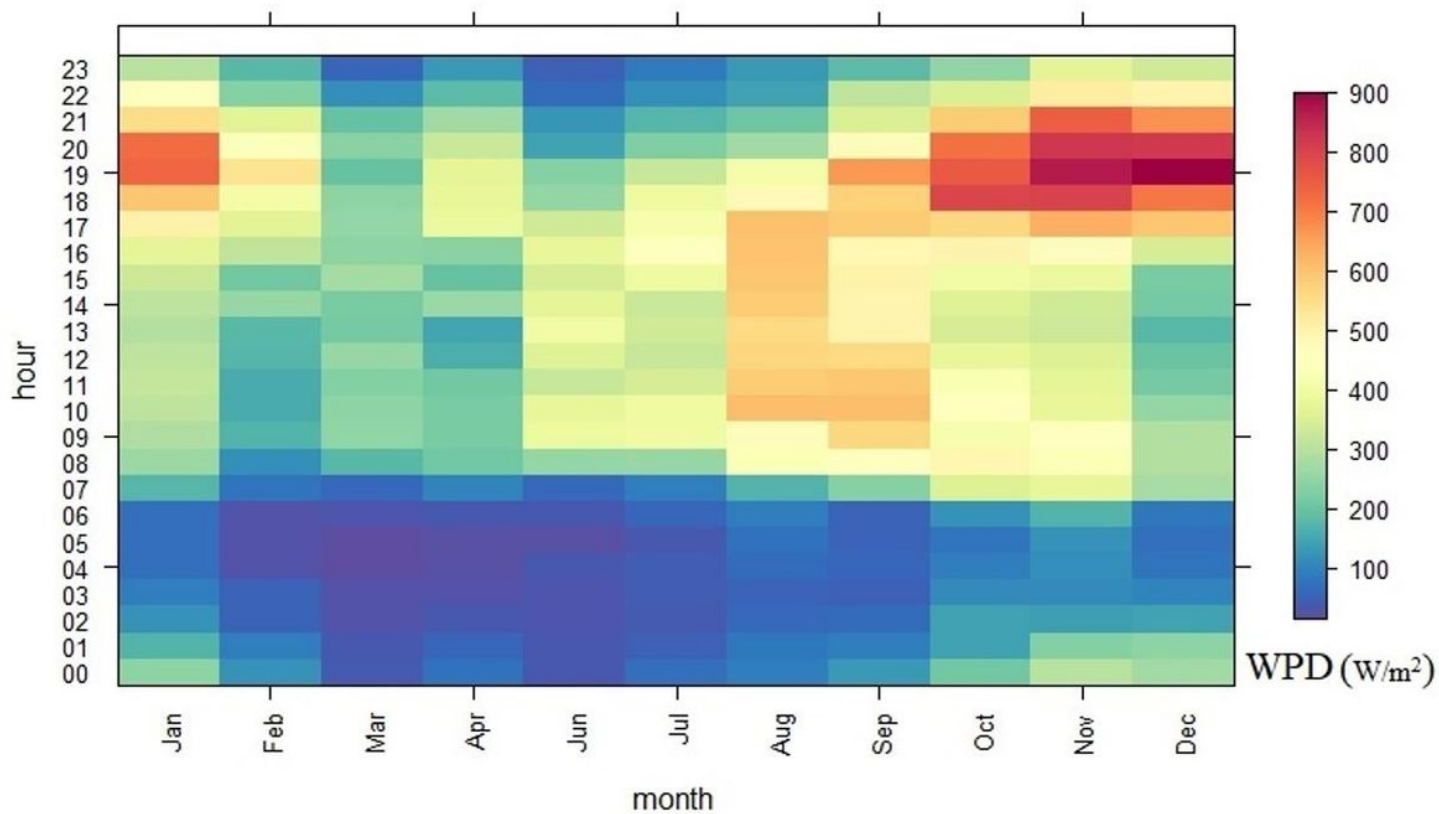


Figure 8

Wind power density (WPD) for the 150 m level.

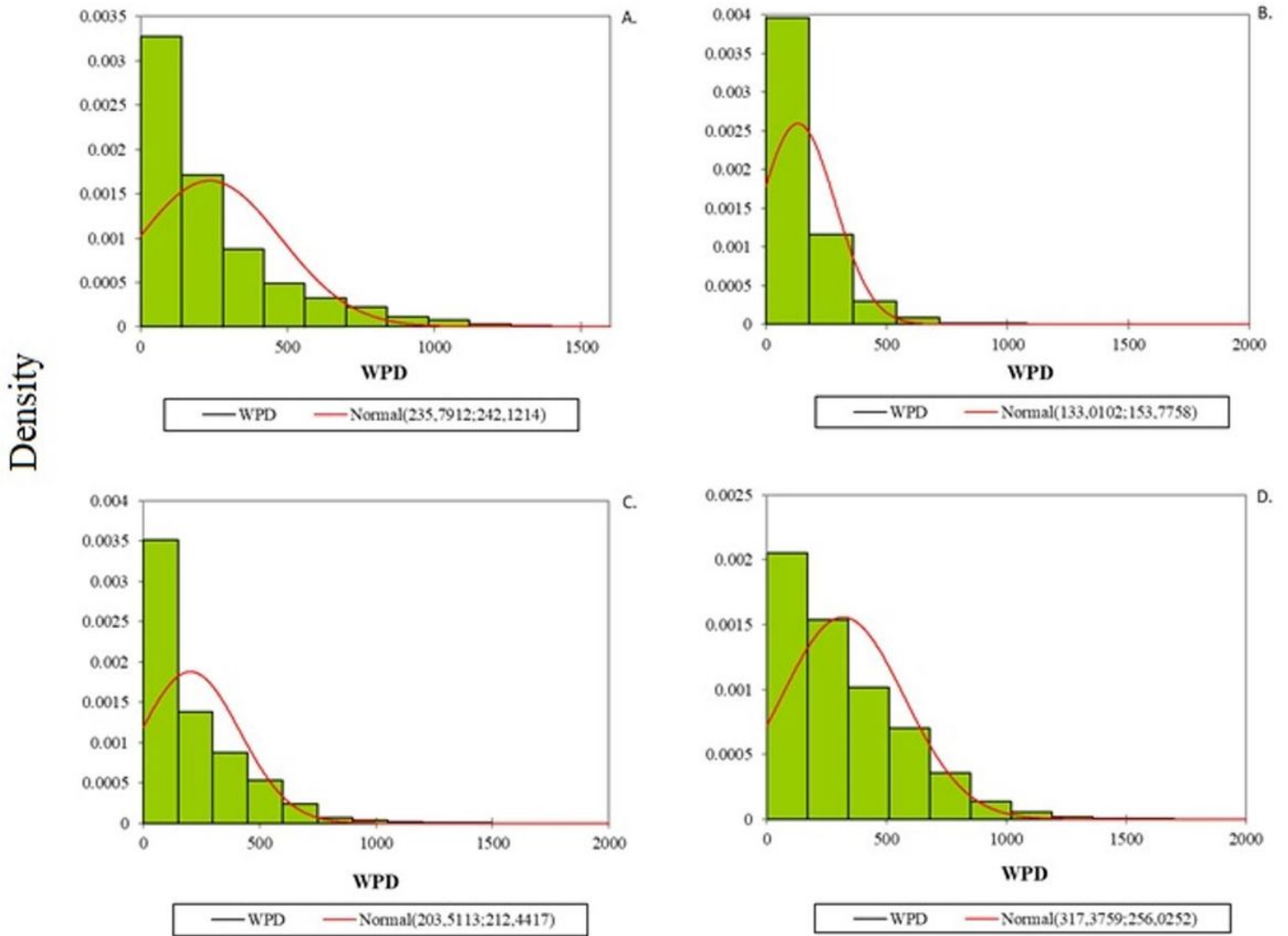


Figure 9

Seasonal distribution of the WPD frequency for the height of 100 m in summer (A), autumn (B), winter (C) and spring (D).

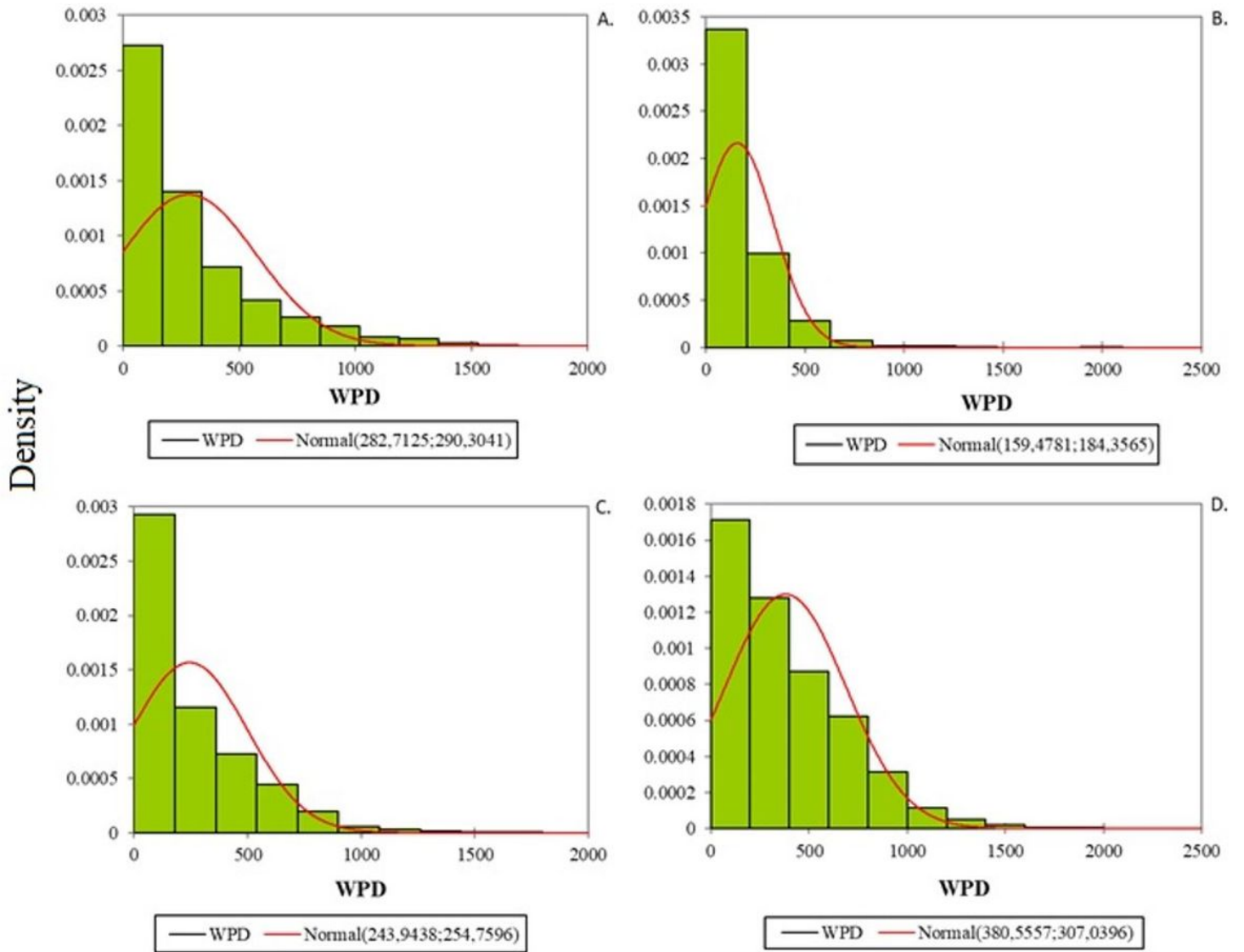


Figure 10

Seasonal distribution of WPD frequency for the height of 150 m in summer (A), autumn (B), winter (C) and spring (D).